

NACA RM L57C14

7753

NACA

Reg # 1458  
APR 25 1957

0144160



# RESEARCH MEMORANDUM

SOME EFFECTS OF HEAT TRANSFER AT MACH NUMBER 2.0  
AT STAGNATION TEMPERATURES BETWEEN 2,310° AND  
3,500° R ON A MAGNESIUM FIN WITH SEVERAL  
LEADING-EDGE MODIFICATIONS

By William M. Bland, Jr., and Walter E. Bressette

Langley Aeronautical Laboratory  
Langley Field, Va.

NATIONAL ADVISORY COMMITTEE  
FOR AERONAUTICS

WASHINGTON  
April 18, 1957



0144160

## NATIONAL ADVISORY COMMITTEE FOR AERONAUTICS

## RESEARCH MEMORANDUM

SOME EFFECTS OF HEAT TRANSFER AT MACH NUMBER 2.0

AT STAGNATION TEMPERATURES BETWEEN 2,310° AND

3,500° R ON A MAGNESIUM FIN WITH SEVERAL

LEADING-EDGE MODIFICATIONS

By William M. Bland, Jr., and Walter E. Bressette

## SUMMARY

Four models of a thin magnesium fin, with the leading edge swept back 35°, of a type used to stabilize the first stages of rocket-propelled multistage hypersonic models have been tested in the pre-flight high-temperature jet of the Langley Pilotless Aircraft Research Station at Wallops Island, Va. This exploratory investigation was made to determine some effects of aerodynamic heating at high stagnation temperatures on the leading edges of fins and to determine the relative effectiveness of several leading-edge protective schemes.

Results of these tests, which were conducted at Mach number 2.0 for various stagnation temperatures between 2,310° and 3,500° R, indicated that under similar test conditions a magnesium fin with a blunt leading edge suffered much less damage than one with a very sharp leading edge even when only the mass remaining after blunting is considered. Also, wrapping sheet Inconel around the leading edge proved to be a very effective scheme for protecting the leading-edge region. Elementary calculations appeared reasonably capable, though conservative, of predicting the time for melting to occur on the Inconel leading edge.

## INTRODUCTION

Problems associated with flight at supersonic speeds have been investigated in free flight by the Langley Pilotless Aircraft Research Division with multistage rocket-propelled models. Conventional fins have been used to stabilize the model-booster combinations at relatively low supersonic speeds. These fins had sharp leading edges to decrease drag and were made of magnesium to decrease the weight. With the advent

~~CONFIDENTIAL~~~~HAAS ADJ 157 3042~~

of research at hypersonic speeds with rocket-propelled models, the velocities attained by the fin-stabilized model-booster combinations have been increased at low altitudes until the aerodynamic heating has become severe enough to be damaging. Recently a large two-stage fin-stabilized model, launched from the ground at about  $55^\circ$  above the horizontal, was accelerated to a Mach number of 2.2 in 4.8 seconds by the first-stage rocket motor. After a short interval of decelerating flight, the model was accelerated by its rocket motor from a Mach number of 1.1 for 2.75 seconds until it unexpectedly underwent an abrupt change in flight path that resulted in model destruction at a Mach number of 4.7 and an altitude of approximately 15,300 feet. Fin failure could have caused the abrupt change in flight path. Subsequent heating calculations were made using the actual flight-path conditions. These calculations indicated that the fin leading edges could have reached the melting temperature of magnesium about 1.5 seconds after the beginning of the second period of acceleration and that the temperature of the magnesium, 3 inches behind the leading edge, could have risen about  $500^\circ$  F by the time of model failure. The results of these calculations thus indicated that the model was probably lost by failure of the fins.

In order to determine some effects of aerodynamic heating at high stagnation temperatures on the leading edge of the fins and to determine the relative effectiveness of several leading-edge protective schemes, an investigation has been initiated by the Langley Pilotless Aircraft Research Division. The first phase of the investigation, as reported herein, was conducted by testing a series of four uninstrumented models of a booster fin in a jet at Mach number 2.0 in which the stagnation temperature could be varied from  $1,200^\circ$  to  $4,000^\circ$  R. In some cases the jet conditions were adjusted so that heating conditions at the fin leading edge were similar to those encountered in free flight by the model previously discussed. These tests were conducted at high stagnation temperatures in the preflight jet of the Langley Pilotless Aircraft Research Station at Wallops Island, Va.

#### MODELS

The plan form chosen for this exploratory investigation simulated the outboard leading-edge portion of a thin booster fin with the relatively small leading-edge half-wedge angle of  $3^\circ$  and the leading edge swept back  $35^\circ$ . Four models (see fig. 1) of this plan form were fabricated from magnesium plate. One, the basic fin, represented the leading-edge region of the full-scale booster fin. The models were modified in the leading-edge region as follows:

~~CONFIDENTIAL~~

- Model 1 . . . . . Basic fin
- Model 2 . . . . . Blunt leading edge
- Model 3 . . . . . Leading edge wrapped with  $\frac{1}{32}$ -inch-thick  
Inconel and blunted as model 2
- Model 4 . . . . . Magnesium leading edge replaced by one machined  
from stainless steel and blunted as model 2

The models were not instrumented.

#### TEST PROCEDURE

The investigation was conducted by exposing the models at a Mach number of 2.0 in the 12-inch-diameter preflight high-temperature jet. Each model was mounted on a stand that would insert and withdraw it from the jet once desired flow conditions had been established. The motion of the stand was such that a model traversed about one-half the jet stream while being rotated to the test position and while being withdrawn. Approximately 0.4 second was spent traversing the jet stream in either direction. Model 2 is shown erected to the testing position, in the center of the jet, in figure 2. The black chordwise line indicates the center of the jet in the vertical plane. A more detailed description of the operation and characteristics of the high-temperature jet is presented in the appendix.

Motion pictures of the model and of an electric clock were taken from one side and from overhead during each test at approximately 128 frames per second. These films provided the only source of data from these tests other than jet operating conditions. From these films were obtained the elapsed time each model was in the testing position and, where applicable, the time at which leading-edge damage was first observed.

#### TESTS AND CALCULATIONS

##### Tests

General.- Calculated stream conditions along the center line of the jet ahead of the model position are presented in figure 3 for different center-line stagnation temperatures. The stagnation temperatures referred to are average values along the center line of the jet for the

~~CONFIDENTIAL~~

~~WDC AD 157-7012~~

time of a test. Variances from the average are quoted for each test in table I.

The tunnel was operated so that the stream static pressure along the center line at the jet exit was 0.78 times the ambient pressure. This resulted in a total pressure of 11,300 pounds per square foot behind a detached shock which is ahead of the  $35^\circ$  sweptback leading edge. An equivalent pressure would be obtained in free flight at Mach numbers 2.6 and 4.0 at altitudes of 20,000 and 40,000 feet, respectively.

Since the jet static pressure was less than ambient, shock diamonds were formed near the exit and extended downstream to intersect several inches behind the leading edges of the models. Information concerning the shock cone is included in the appendix.

Test times given are for the interval of time a model was exposed to the jet in the testing position. Other pertinent information concerning the tests is included in table I.

Model 1, basic fin. - The basic magnesium fin with the very sharp leading edge ( $1/64$ -inch radius) was inserted in the jet with the stagnation temperature at  $2,390^\circ$  R. Melting of the wing leading edge was observed to start near the jet center line at 0.6 second. Damage after exposure for 2.3 seconds was extensive as shown in figure 4. As a matter of interest, the calculated heat input to the fin leading edge during the 2.3-second test was of the same order as that calculated for the flight condition discussed in the "Introduction."

Model 2, blunt leading edge. - The magnesium fin with the leading edge blunted to a  $1/16$ -inch radius was inserted in the jet with the stagnation temperature at  $2,310^\circ$  R. Melting of the wing leading edge was observed to start slightly above the jet center line at 1.9 seconds which is considerably later than the time melting was observed to start on the basic fin. Damage after exposure for 2.3 seconds was relatively small as shown in figure 5. The benefit derived by blunting the leading edge is shown quite clearly by a comparison between figures 4 and 5. The black line extending from root to tip just behind the leading edge of model 1 (basic fin) in figure 4, which shows the relative position of the leading edge of model 2 (fig. 5), is indicative of the amount of material removed from the basic fin to arrive at model 2. Thus for approximately similar test conditions the fin with the sharp leading edge sustained more damage than the fin with the blunt leading edge even when only the reduced mass of model 2 is considered. That is, damage to the fin with the sharp leading edge extended farther behind a line representing the leading edge of model 2 than the damage to model 2. The stagnation temperatures of these tests,  $2,390^\circ$  and  $2,310^\circ$  R, compare approximately with the stagnation temperatures that would be obtained in flight at Mach numbers 5.0 and 4.9, respectively, at an altitude of 40,000 feet. (See table I.)

~~CONFIDENTIAL~~

Model 3, blunt leading edge wrapped with Inconel.- The fin with the 1/32-inch-thick Inconel wrapped around the leading edge was exposed in the jet at conditions slightly more severe than those of the previous tests (2.3 seconds at a stagnation temperature of 2,540° R) without damage. In subsequent tests the fin was exposed for 2.4 seconds at 2,910° R and for 2.3 seconds at 3,220° R. The Inconel was held in place by rivets as indicated in figure 1. Prior to the tests, considerable concern was expressed on the possible effectiveness of this type of attachment because of the different coefficients of thermal expansion of Inconel and magnesium. Examinations after each of these tests disclosed only minor effects such as Inconel discoloration, deformation of the rivet heads, and some Inconel buckling between the rivets. The extent of each of these effects of heating increased as the stagnation temperature increased. No evidence of damage to the exposed magnesium surfaces was observed during or after these three tests.

Model 3 was finally tested in the jet with the stagnation temperature at 3,500° R, the maximum stagnation temperature available at the time of the investigation. After exposure for about 2.5 seconds the Inconel melted at the leading edge near the jet center line and the magnesium appeared to ignite under the Inconel and immediately behind the Inconel on the side of the fin. Total time in the testing position was 3.2 seconds. Damage to the leading edge and the rest of the fin is shown in figure 6.

Model 4, blunt leading edge made of stainless steel.- This model, which had the magnesium replaced by stainless steel at the leading edge and for a considerable distance behind the leading edge (see fig. 1) was tested at a stagnation temperature of 3,500° R. It was tested at only this stagnation temperature because experience with model 3 indicated that model 4 would survive exposure at the lower stagnation temperatures. At about 2.5 seconds, as in the test of model 3 at the same stagnation temperature, the magnesium was observed to ignite near the jet center line immediately to the rear of the stainless steel, which was red hot where it joined the magnesium. Total time in the testing position was 3.7 seconds. The stainless-steel leading edge was undamaged during the test; however, considerable damage was sustained by the magnesium behind the stainless-steel section as can be seen in figure 7. The stagnation temperature of 3,500° R of the last test of model 3 and of the test of model 4 is comparable to the stagnation temperature that would be obtained at a Mach number of 6.3 at an altitude of 40,000 feet.

Some idea of the relative effectiveness of the three leading-edge protective schemes can be obtained from figure 8 and from table I.

The first damage observed during some of the tests was melting of the magnesium; in other tests ignition of the magnesium was the first damage observed. According to reference 1, magnesium could be expected to ignite near the melting temperature; therefore, the appropriate test times for which ignition was first observed are taken as times for melting to begin.

## Calculations

Heating calculations at the leading edge, on the 1/32-inch-thick Inconel, and at a station 2.5 inches behind the leading edge, on 0.17-inch-thick magnesium, have been made for model 3 at a stagnation temperature of 3,500° R by using simple heat balance relations. General assumptions made in performing these calculations are as follows:

1. No temperature gradients along the surface or through the material
2. No radiation

Assumptions made in performing the calculations at the leading edge are as follows:

1. Flow is laminar
2. Adiabatic wall temperature equal to the stagnation temperature
3. Effective thickness of Inconel was taken as 74.8 percent of sheet thickness. This resulted from dividing the volume of the material by the surface area to obtain an average thickness.
4. No conduction to the magnesium enclosed by the Inconel

Assumptions made in performing the calculations behind the leading edge are as follows:

1. Turbulent flow existed from the leading edge
2. Van Driest's values of the turbulent flat-plate skin friction were applicable
3. Reynold's analogy constant was 0.6.
4. Recovery factor was equal to the cube root of the Prandtl number based on wall temperature.

Average aerodynamic heat-transfer coefficients for the leading-edge calculations were calculated by the method of reference 2 for a two-dimensional body.

Calculated wall temperatures at the leading edge and at a station 2.5 inches behind the leading edge are shown in figure 9. The temperature calculations at the leading edge on the Inconel appear to be conservative, that is, melting was calculated to occur at 2.0 seconds while actual fin failure was observed to occur at the later time of 2.5 seconds. This conservatism in the calculation of the temperature of Inconel is influenced by the assumption of no conduction and by the assumption of no radiation.

It should also be noted that, although this conservative calculation failed to predict the time of model failure from Inconel melting by a considerable fraction of the total test time, the actual error in heat input was only about 10 percent of the total heat required to raise Inconel to its melting temperature.

The calculated melting time for the magnesium (2.5 in. behind the leading edge) was nearly 4.4 seconds. This, when compared with the observed fin failure time of about 2.5 seconds supports the observation made in the previous section that first failure on the fin occurred on the Inconel.

Calculated heating rates are presented in figure 10 to give some idea of the severity of these tests. These heating rates are somewhat disproportionate; that is, under the artificial test conditions of the high-temperature jet, the heating rate at the leading edge may not be related to the heating rate behind the leading edge on the wing surface in the same manner as it would be in free flight. For instance, at a stagnation temperature of 3,500° R, the calculated heating rate at the leading edge is less than that calculated for altitudes of 50,000 feet and under. On the other hand, the calculated heating rate on the surface of the fin 2.5 inches behind the leading edge is less than that calculated for altitude of 30,000 feet and under. Thus, for many tests in the jet it is possible that the heating behind the leading edge may become too severe when some leading-edge conditions are reproduced. This discrepancy exists because the Mach number in the jet cannot be varied to complete the simulation of the leading-edge conditions.

### CONCLUSIONS

Results of seven tests of four models of a magnesium fin, three with modifications designed to alleviate heating effects in the leading-edge region, in a high-temperature jet at Mach number 2.0 indicate the following conclusions:

1. Under similar test conditions, a magnesium fin with a blunt leading edge suffered much less damage than one with a very sharp leading edge even when only the mass remaining after blunting was considered.
2. Wrapping Inconel around the leading edge, while a very simple modification, proved to be a very effective scheme for protecting the leading-edge region.



3. Elementary calculations appeared reasonably capable, though conservative, of predicting the time for melting of an Inconel leading edge.

Langley Aeronautical Laboratory,  
National Advisory Committee for Aeronautics,  
Langley Field, Va., March 4, 1957.

## APPENDIX A

## HIGH-TEMPERATURE JET

In order to study high-temperature effects on components of missiles expected to obtain hypersonic speeds, it became necessary to develop a ground-test jet capable of producing high-temperature flow associated with hypersonic speeds. This high-temperature jet was obtained by ducting air from the storage spheres of the preflight test facilities of the Langley Pilotless Aircraft Research Division (ref. 3) through a fuel spray and flame-holder donut-type burner where ethylene vapor fuel ( $C_2H_4$ ) is injected into the airstream. The resulting combustible mixture is then ignited and burned in a combustion chamber with the products of combustion exhausted into the atmosphere through a convergent-divergent exit nozzle at Mach number 2. A schematic drawing showing the internal characteristics of the jet ducting and the Mach cone is presented in figure 11. Also shown in figure 11 is the operation of the swing mechanism used for inserting the test models into the hot jet after the jet has reached steady-state conditions. The stagnation temperature of the jet exhaust can be varied from the preheat values of the air supply by regulating the fuel supply, whereas the static pressure at the nozzle exit is controlled by regulation of the total pressure upstream of the burner. The calculated variation in temperature with fuel supplied is presented in figure 12. The adiabatic equilibrium flame temperature after burning ethylene ( $C_2H_4$ ) fuel with fuel-air ratio was computed from data presented in reference 4. Calibration of the exhaust-temperature profiles across the nozzle exit at various injection values of fuel and air supply was obtained up to a value of  $2,700^\circ R$  by a temperature survey rake stationed at  $45^\circ$  across the exit. Typical stagnation-temperature profiles obtained with the temperature rake are presented in figure 13. Figure 13 shows that the stagnation temperature is not constant across the nozzle exit of the jet and that the maximum for any test is near the center line of the jet. Also as the center-line stagnation temperature increased, the temperature gradient from the center to the nozzle wall increased. For center-line stagnation temperature near  $2,300^\circ R$ , the temperature gradient was about  $100^\circ$  per inch near the center line. Because center-line stagnation temperature above  $2,700^\circ R$  could not be measured in the calibration of the jet, any center-line value above  $2,700^\circ R$  must be estimated by extrapolation of the values of the stagnation temperature and fuel-air ratio.

Presented in figure 14 is the percent by weight of the ethylene exhaust-gas products for fuel-air ratios less than the stoichiometric value. The values of the exhaust-gas products were computed by the method presented in appendix B of reference 5 with the assumption that

~~CONFIDENTIAL~~

the hydrogen-carbon fuel ( $C_2H_4$ ) is completely converted to carbon dioxide and water vapor. It can be seen in figure 14 that the percent-by weight of nitrogen in the gas is reduced by only 6 percent from a value of 77 percent for air to a value of 71 percent for the-exhaust at the stoichiometric value. The fact that the nitrogen content of the exhaust is large and fairly consistent with the nitrogen content of air indicates that the heat transfer from the high-temperature exhaust should be closely similar to the heat transfer at high temperatures from air. However, the reduction in oxygen with the resultant increase in carbon dioxide and water may alter substantially the surface chemistry phenomena at high temperature.

It is also necessary to have some idea of the thermodynamic properties of the exhaust mixture. Although these thermodynamic properties, such as gas constant  $R$ , specific heat at constant pressure  $c_p$ , and ratio of specific heats  $\gamma$ , might vary slightly for different runs, a reasonable engineering estimate can be computed by a weighted averaging process for the values of temperature with fuel-air ratio as presented in figure 15 by using data presented in references 4 and 5 for the thermodynamic properties of each of the exhaust products with temperature. The computed values for  $c_p$  and  $\gamma$  are presented in figure 15 whereas figure 5 of reference 5 shows, for the combustion of ethylene fuel which has a hydrogen-carbon ratio of 0.168, that  $R$  remains approximately  $53.3 \frac{\text{ft-lb}}{\text{lb } ^\circ\text{F}}$  over a range of fuel-air ratio from 0 to the stoichiometric value. Also presented in figure 15 are the  $c_p$  and  $\gamma$  variations with temperature for air as obtained from references 6 and 7. It can be seen in figure 15 that the thermodynamic properties of the exhaust gas are very similar to those of air.

Thus, from the results presented in this appendix, it can be expected that tests of aerodynamic shapes in the high-temperature jet simulate tests in the atmosphere under similar temperature conditions.

## REFERENCES

1. Hill, Paul R., Adamson, David, Foland, Douglas H., and Bressette, Walter E.: High-Temperature Oxidation and Ignition of Metals. NACA RM L55L23b, 1956.
2. Goodwin, Glen: Heat-Transfer Characteristics of Blunt Two- and Three-Dimensional Bodies at Supersonic Speeds. NACA RM A55L13a, 1956.
3. Faget, Maxime A., Watson, Raymond S., and Bartlett, Walter A., Jr.: Free-Jet Tests of a 6.5-Inch-Diameter Ram-Jet Engine at Mach Numbers of 1.81 and 2.00. NACA RM L50L06, 1951.
4. Fricke, Edwin F.: Statistical Thermodynamics Applied to Chemical Kinetics of Combustion. Rept. No. EDR-22-407, Republic Aviation Corp., Oct. 1, 1947.
5. Pinkel, Benjamin, and Turner, L. Richard: Thermodynamic Data for the Computation of the Performance of Exhaust-Gas Turbines. NACA WR E-23, 1944. (Formerly NACA ARR 4B25.)
6. Hilsenrath, Joseph, Beckett, Charles W., et al.: Tables of Thermal Properties of Gases. NBS Cir. 564, U. S. Dept. Commerce, 1955.
7. Ames Research Staff: Equations, Tables, and Charts for Compressible Flow. NACA Rep. 1135, 1953. (Supersedes NACA TN 1428.)

~~CONFIDENTIAL~~

TABLE I

## SUMMARY OF TEST CONDITIONS AND RESULTS

[The tests were conducted so that the total pressure behind a detached shock ahead of the fin leading edge was 11,300 pounds per square foot which is representative of the pressure obtained at a Mach number of 2.6 at an altitude of 20,000 feet or at a Mach number of 4.0 at an altitude of 40,000 feet.]

Model	Stagnation temperature, $^{\circ}\text{R}$	Temperature variation, $^{\circ}\text{R}$	Percent of oxygen by volume of total gases in exhaust	Equivalent Mach no. at sea level (a)	Equivalent Mach no. at 40,000 ft (a)	Test duration, sec	Time of failure, sec	Remarks
1	2,390	$\pm 10$	13.0	4.2	5.0	2.3	0.6	{ Excessive damage to leading edge
2	2,310	$\pm 15$	13.5	4.1	4.9	2.3	1.9	{ Some damage to leading edge
3	2,540	$\pm 61$	12.6	4.6	5.4	2.3	---	{ Very small buckles in Inconel
3	2,910	$\pm 40$	10.4	4.9	5.7	2.4	---	{ Large buckles in Inconel
3	3,220	$\pm 100$	8.7	5.2	6.0	2.3	---	{ Very large buckles in Inconel
3	3,500	$\pm 100$	7.3	5.5	6.3	3.2	2.5	{ Excessive damage to Inconel leading edge; magnesium parts burned
4	3,500	$\pm 100$	7.3	5.5	6.3	3.7	2.5	{ Excessive damage; magnesium parts burned; stainless-steel leading edge undamaged

<sup>a</sup>Equivalent Mach number is the one that gives the stagnation temperature of the test at indicated altitude.

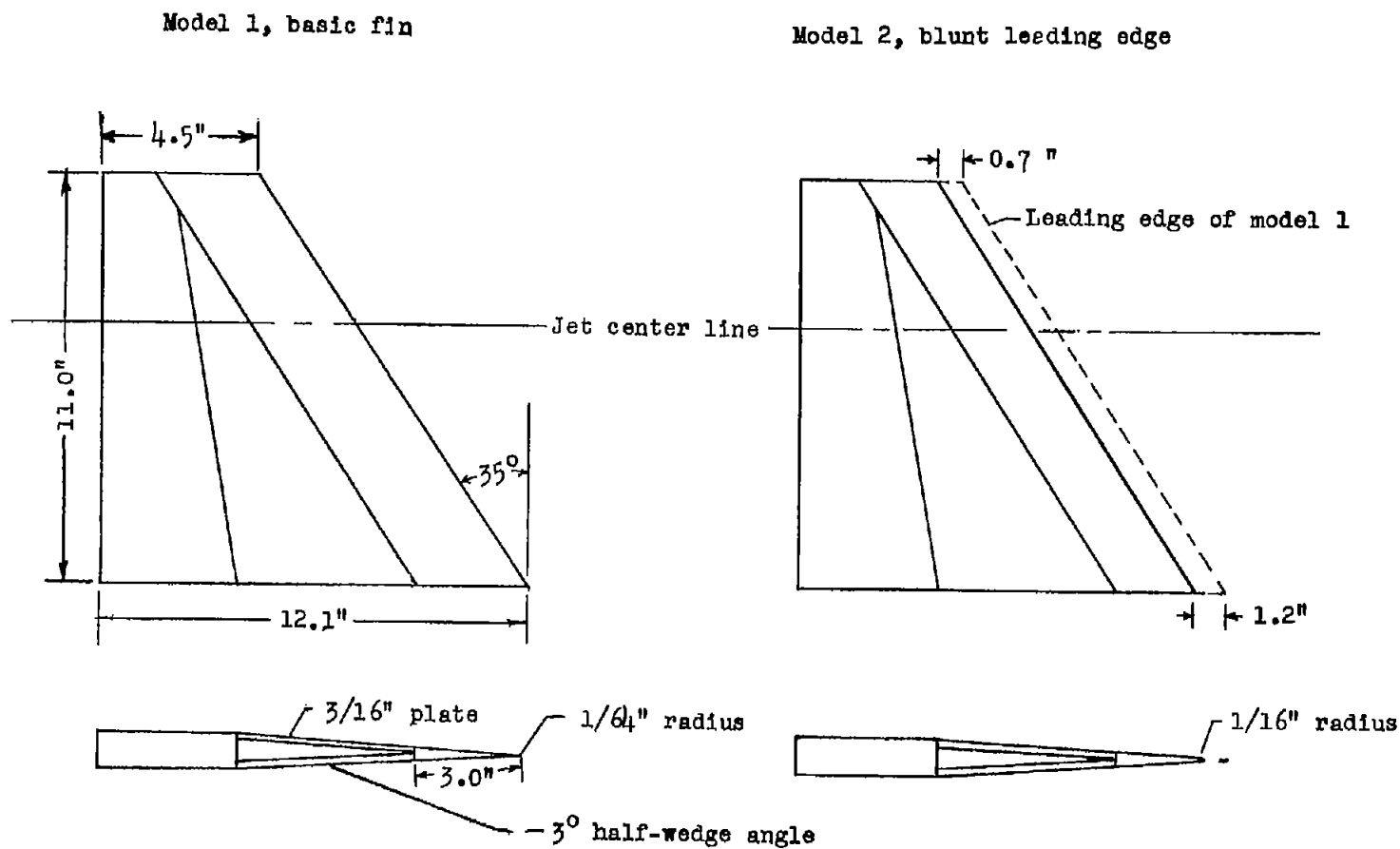
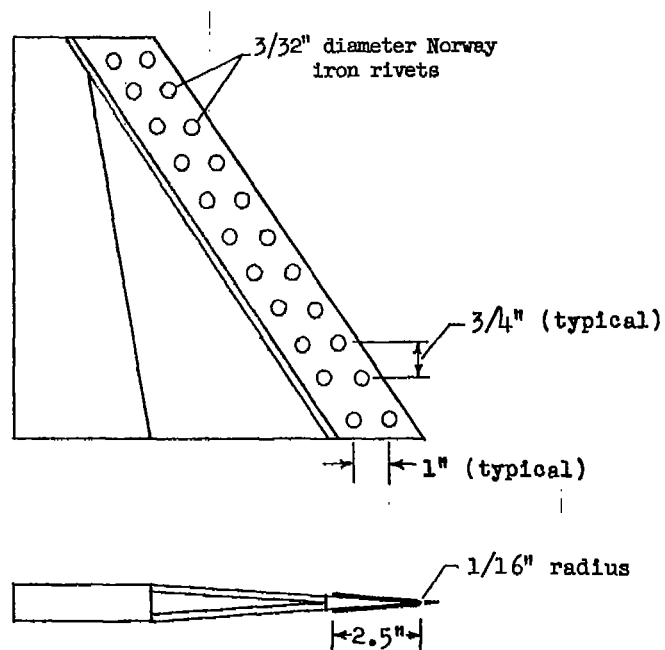


Figure 1.- General features of the models.

Model 3, blunt leading edge wrapped with  
1/32-inch thick Inconel



Model 4, blunt leading edge made  
of stainless steel

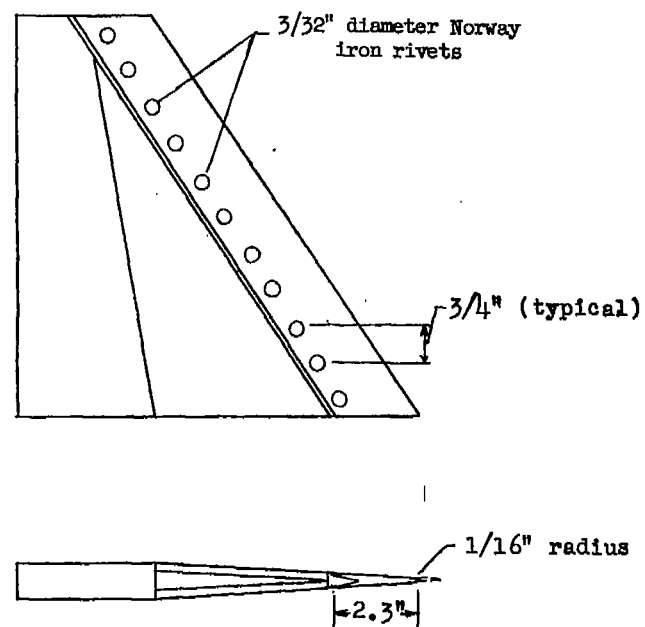


Figure 1.- Concluded.

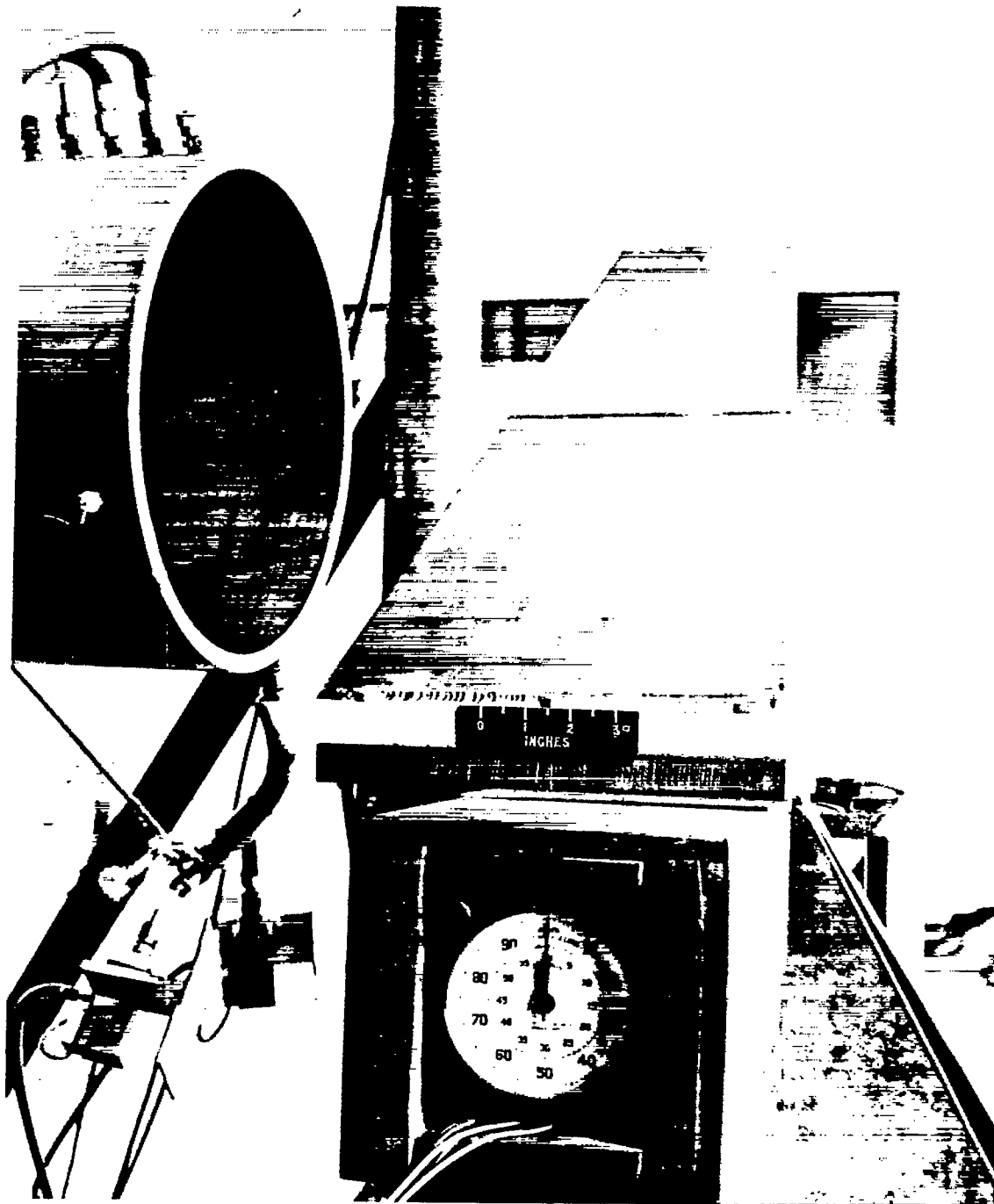
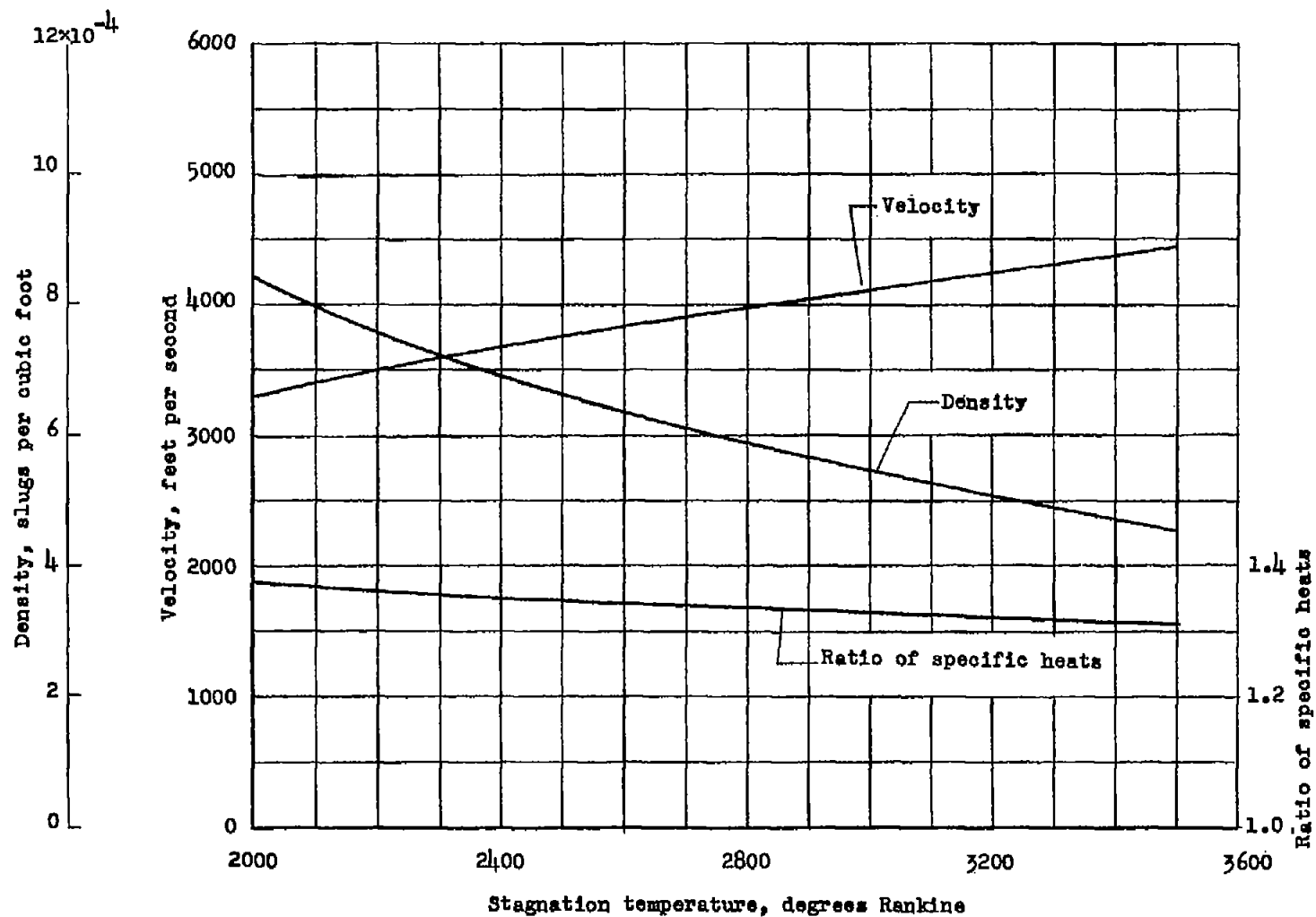


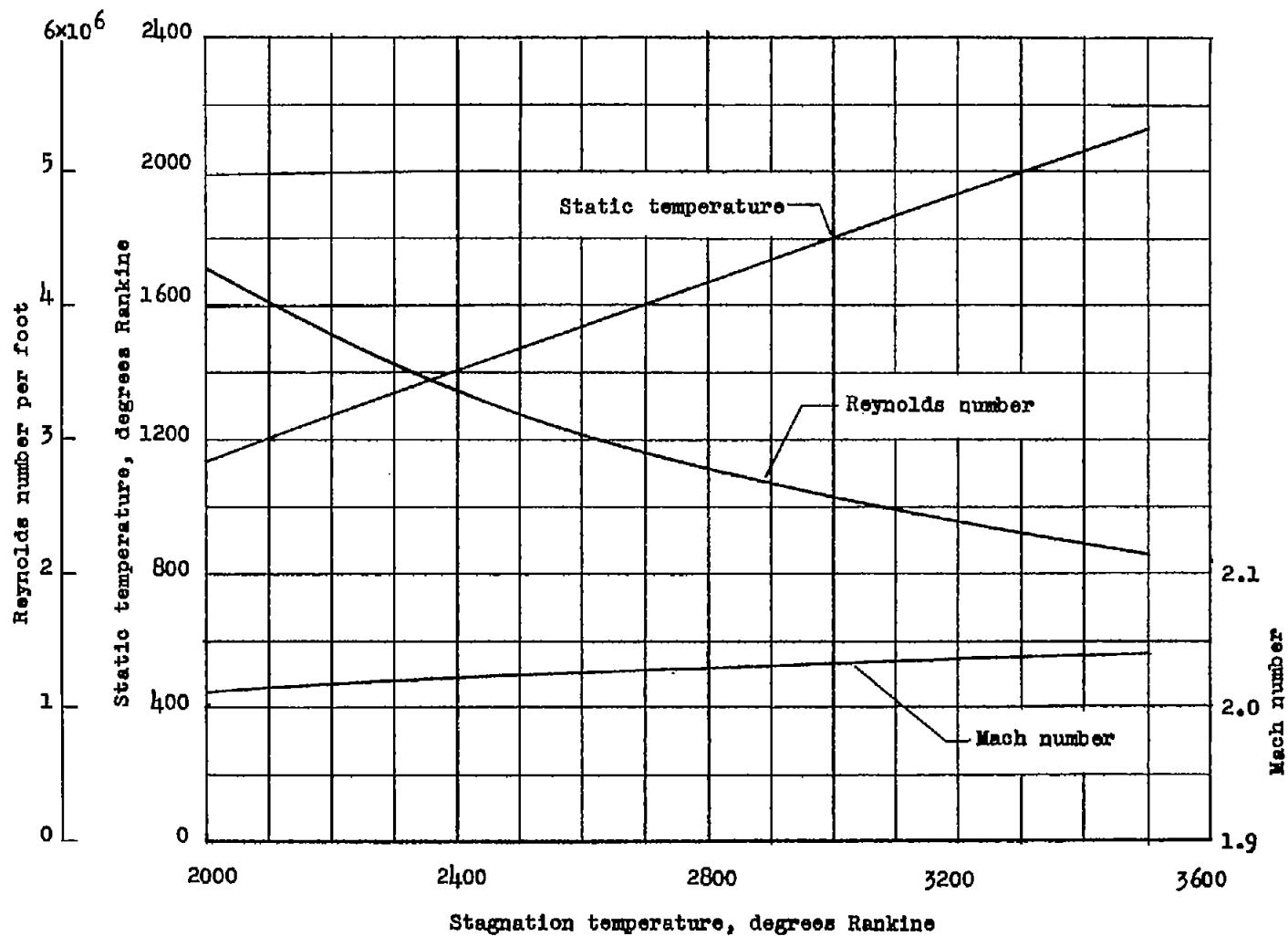
Figure 2.- Model 2 in the testing position. L-93488.1





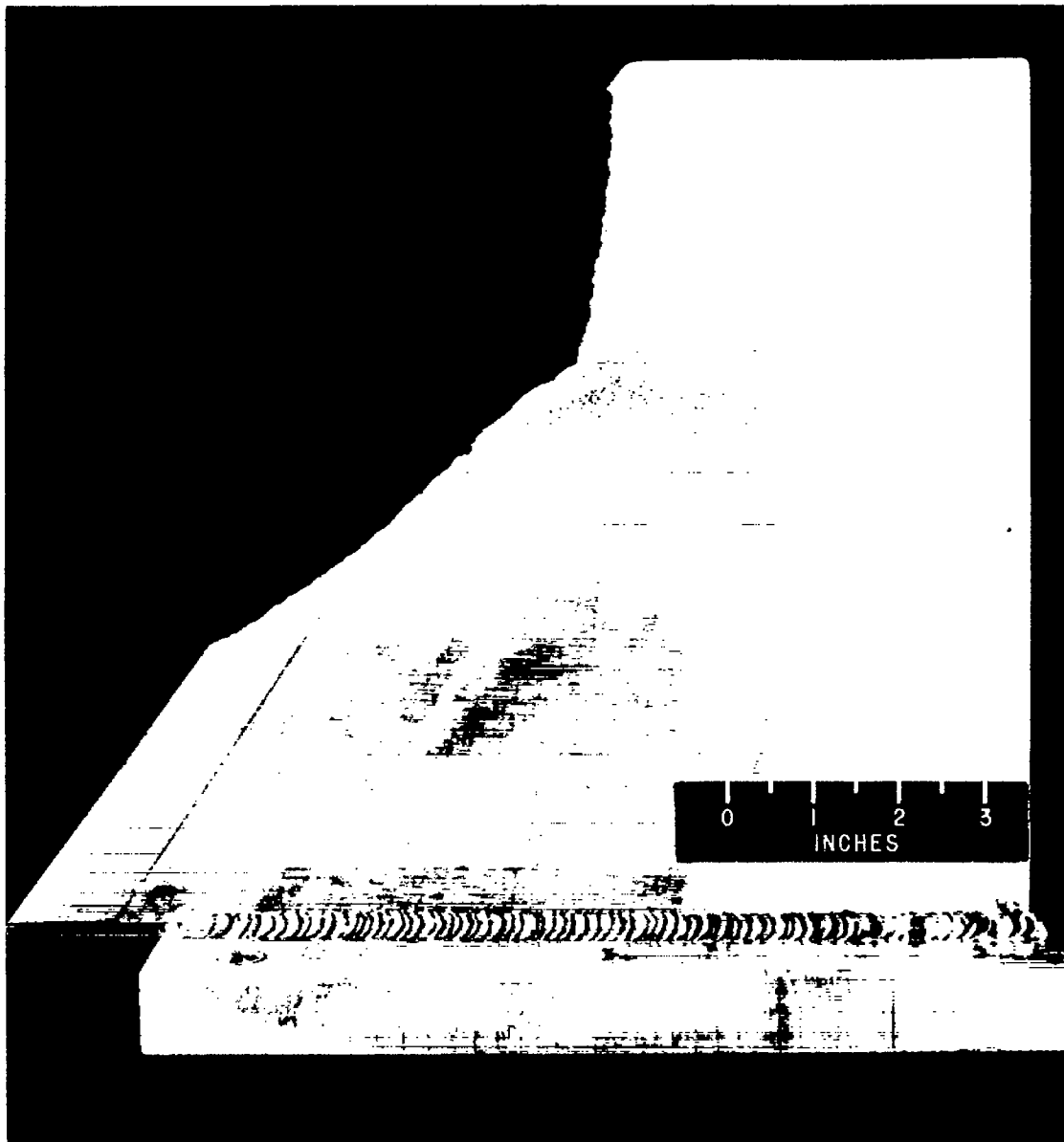
(a) Velocity, density, and ratio of specific heats.

Figure 3.- Variation of stream conditions along jet center line with stagnation temperature.



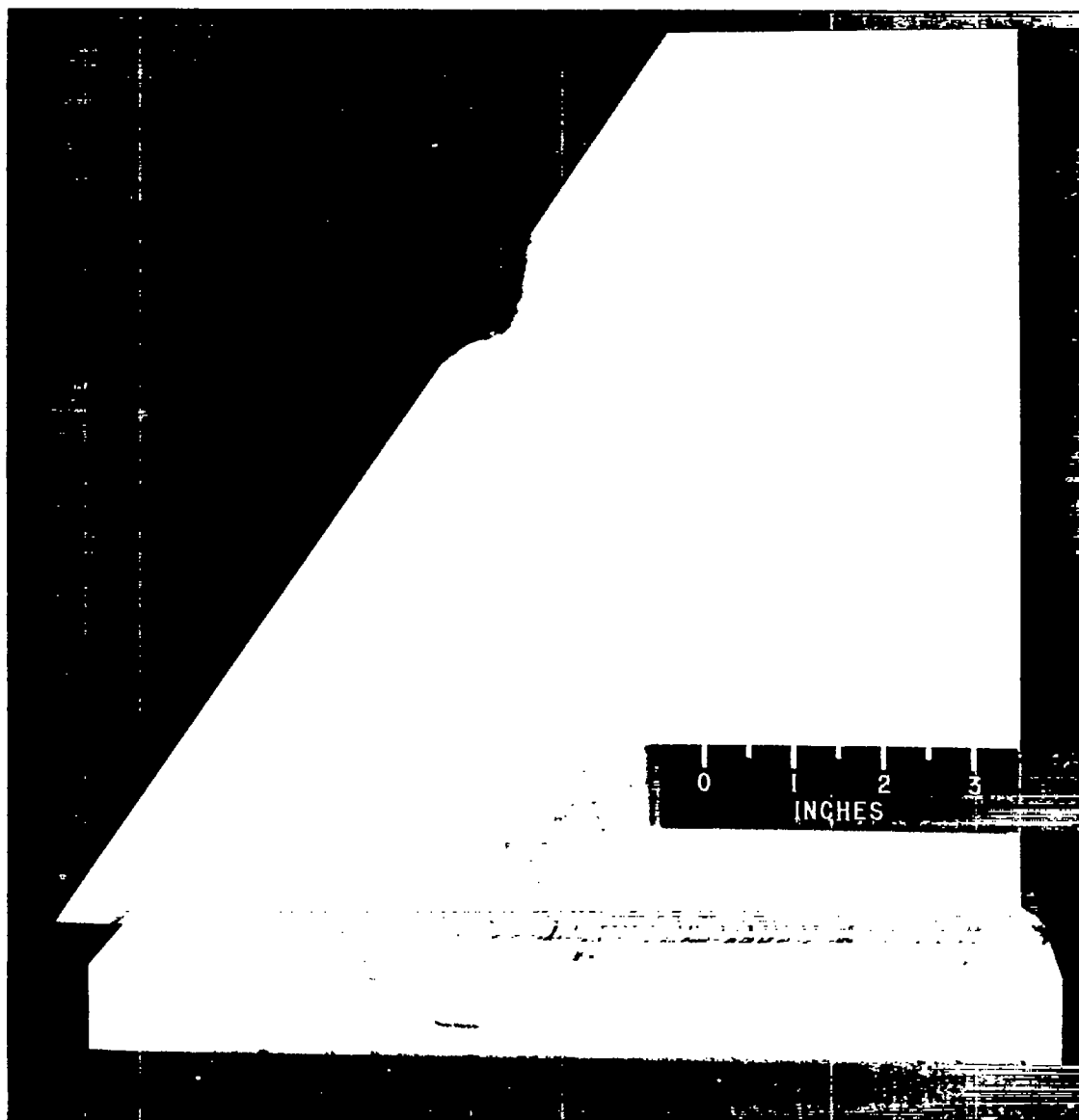
(b) Reynolds number per foot, static temperature, and Mach number.

Figure 3.- Concluded.



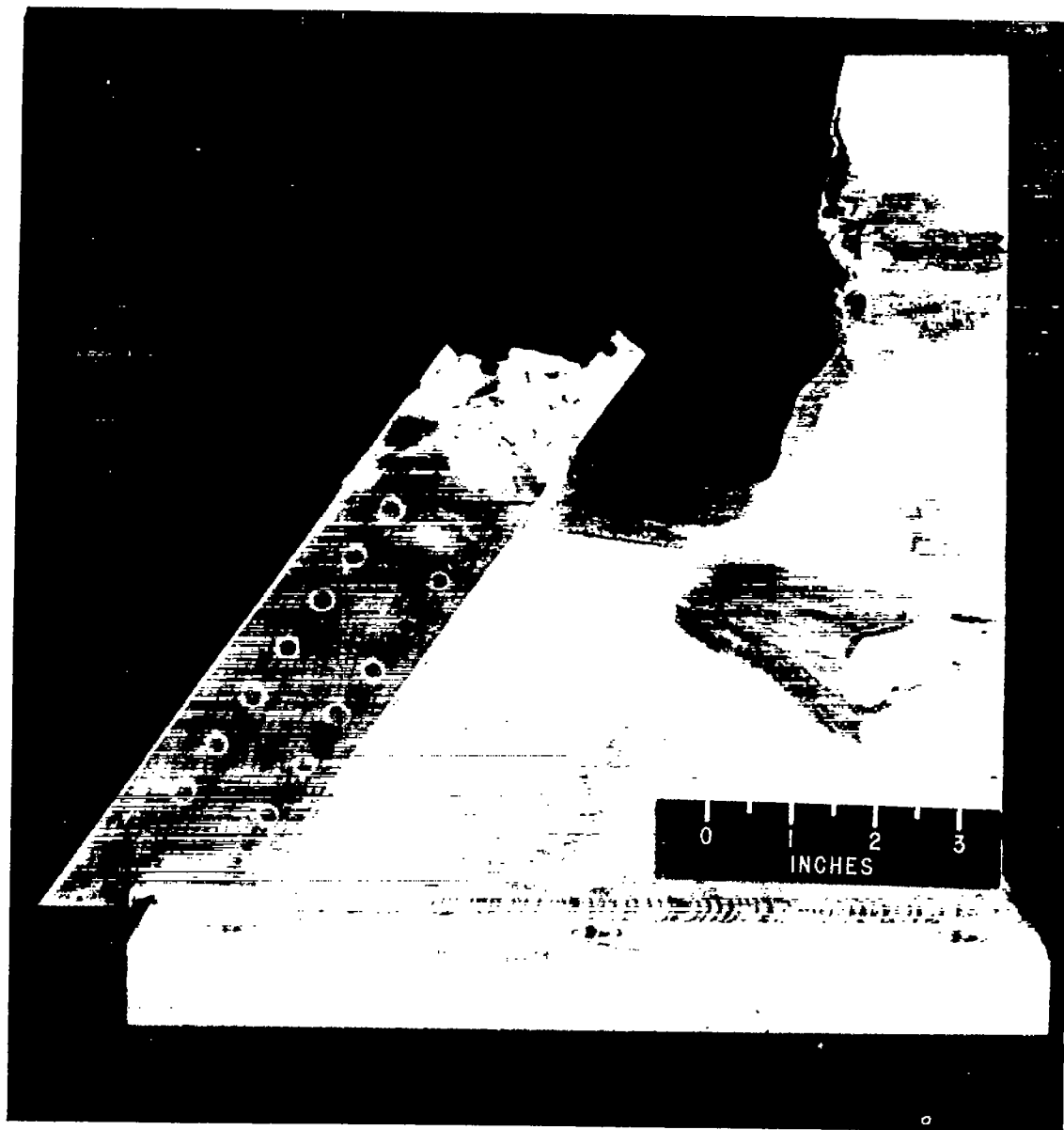
L-93486.1

Figure 4.- Damage to the leading edge of model 1 after exposure for 2.3 seconds at  $2,390^{\circ}$  R.



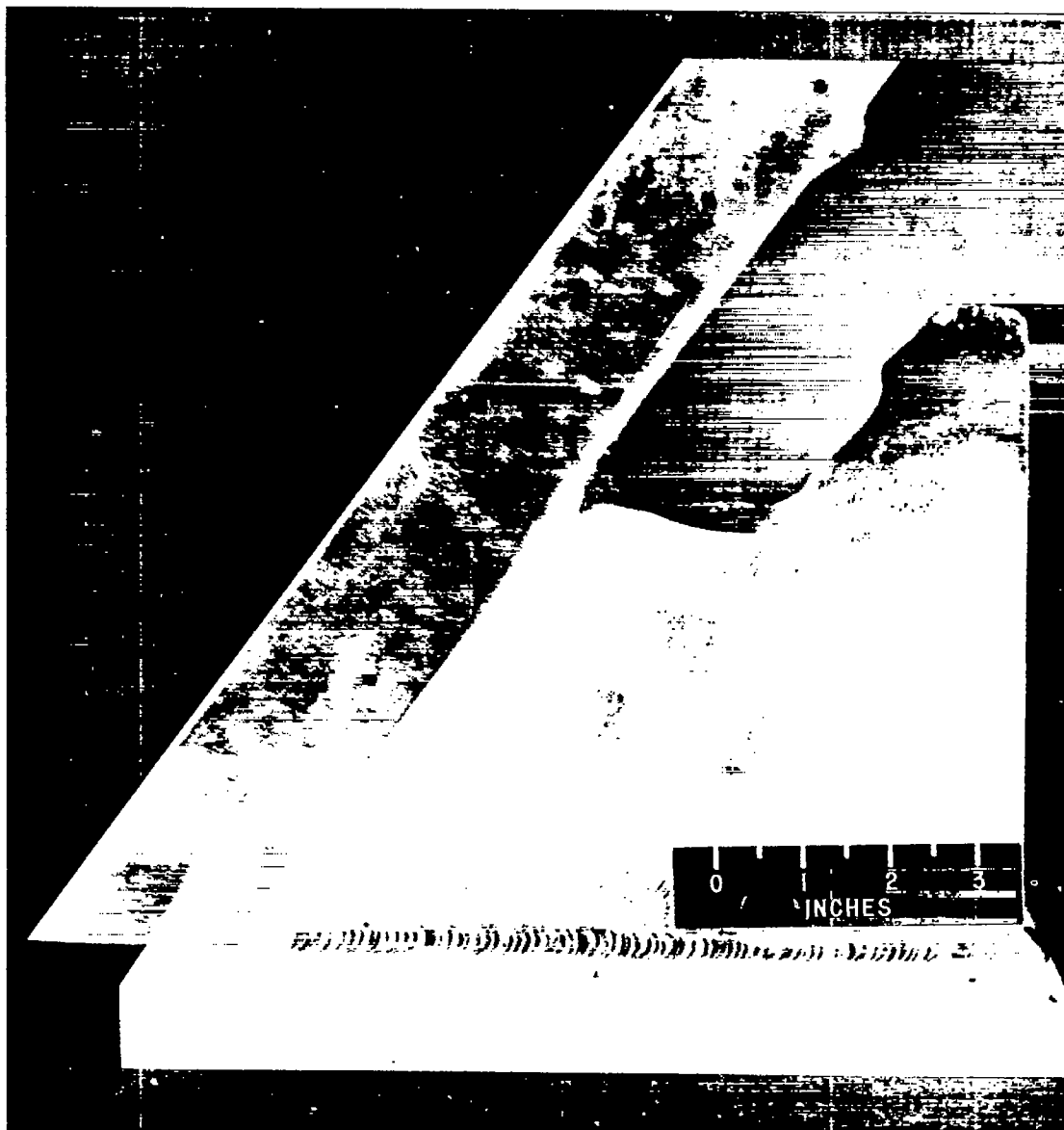
L-93485.1

Figure 5.- Damage to the leading edge of model 2 after exposure for 2.3 seconds at  $2,310^{\circ}$  R.

~~CONFIDENTIAL~~

L-93489.1  
Figure 6.- Damage to model 3 after exposure for 3.2 seconds at 3,500° R.

~~CONFIDENTIAL~~



L-93490.1

Figure 7.- Damage to model 4 after exposure for 3.7 seconds at  $3,500^{\circ}$  R.

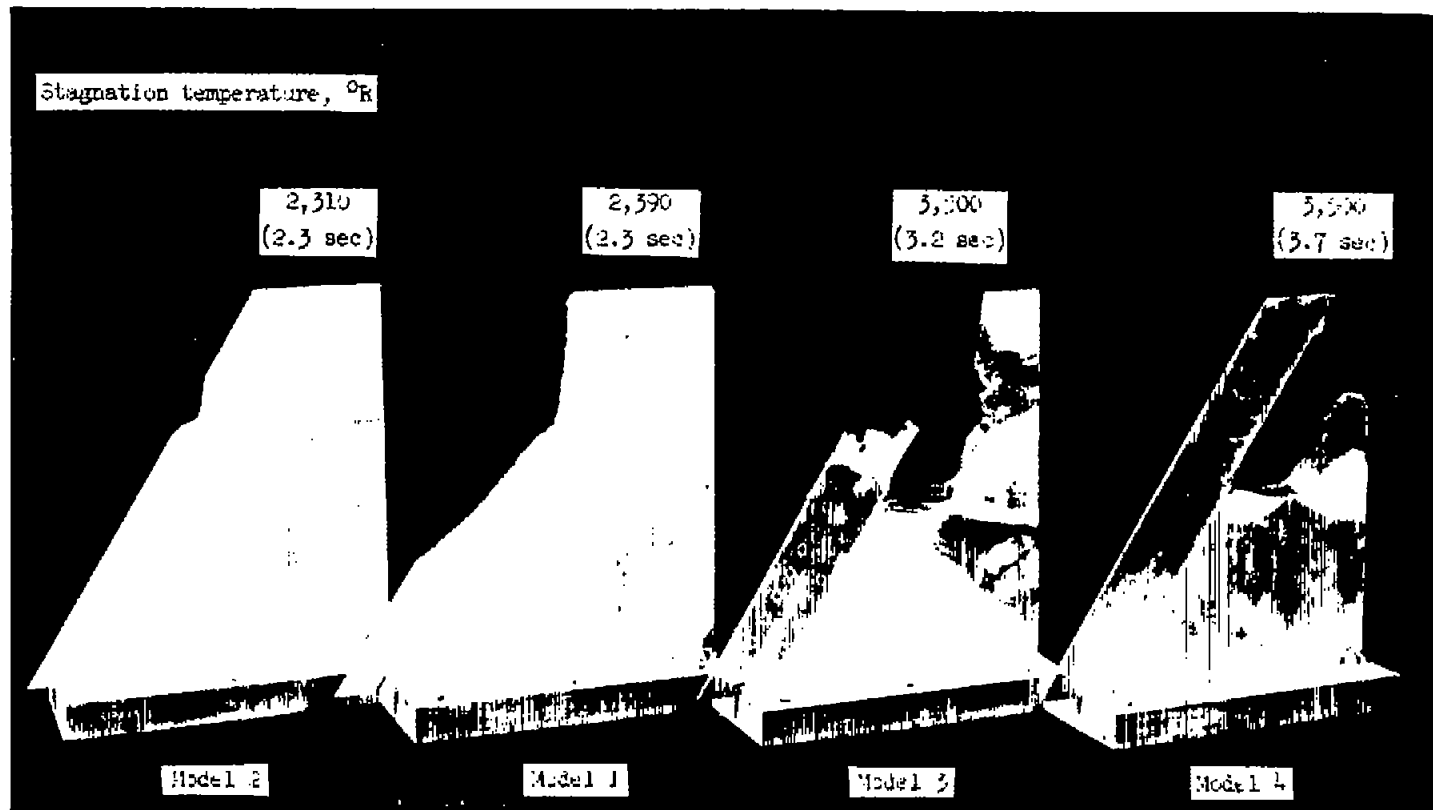


Figure 8.- Damage to all models under indicated conditions. L-93484.1

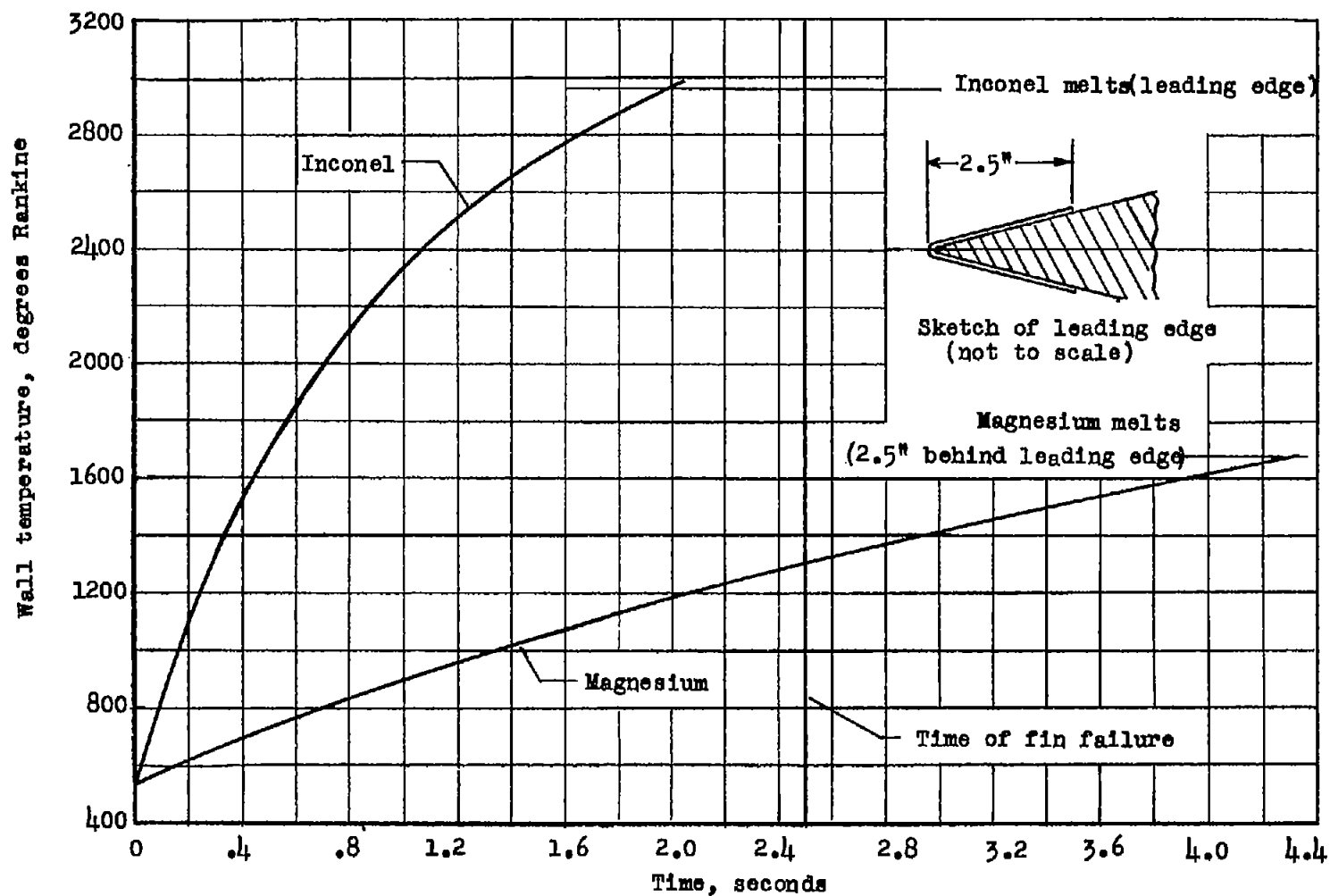


Figure 9.- Calculated wall temperature at the leading edge and on the surface 2.5 inches behind the leading edge of model 3 for a stagnation temperature of  $3,500^{\circ}$  R.



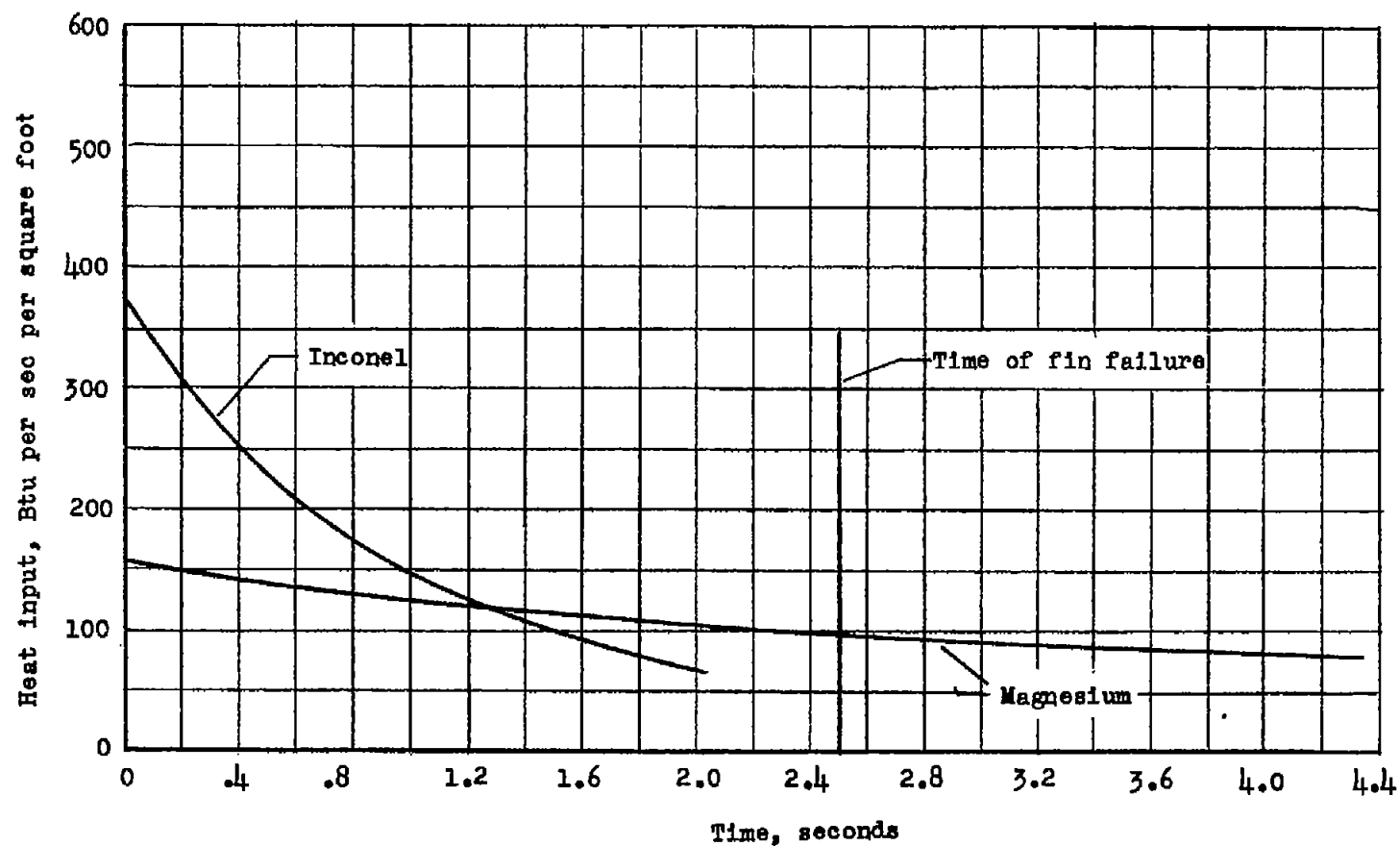


Figure 10.- Calculated heat input to the leading edge and to the surface 2.5 inches behind the leading edge of model 3 for a stagnation temperature of  $3,500^{\circ}$  R.

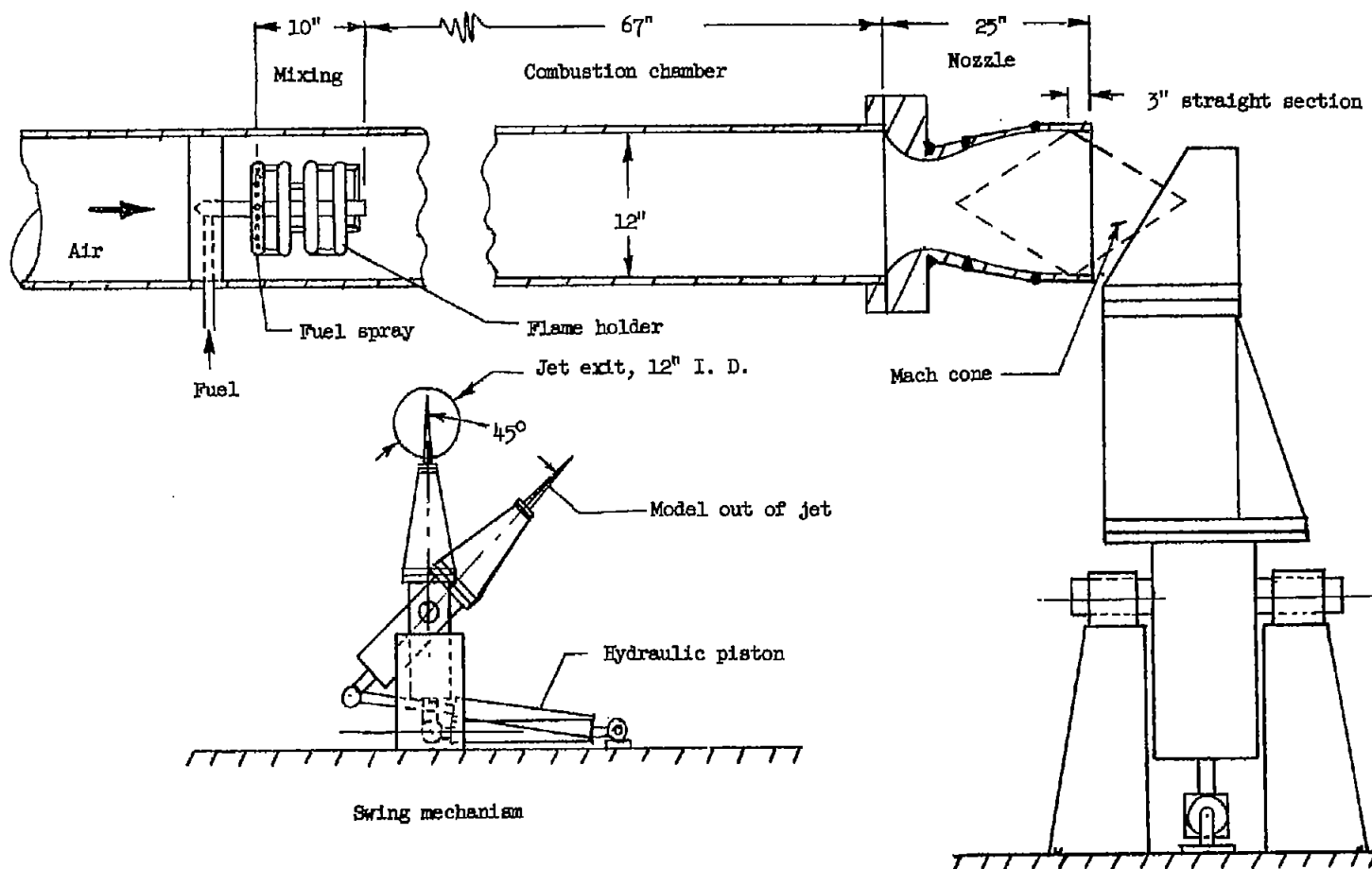


Figure 11.- Schematic drawing of preflight high-temperature jet.

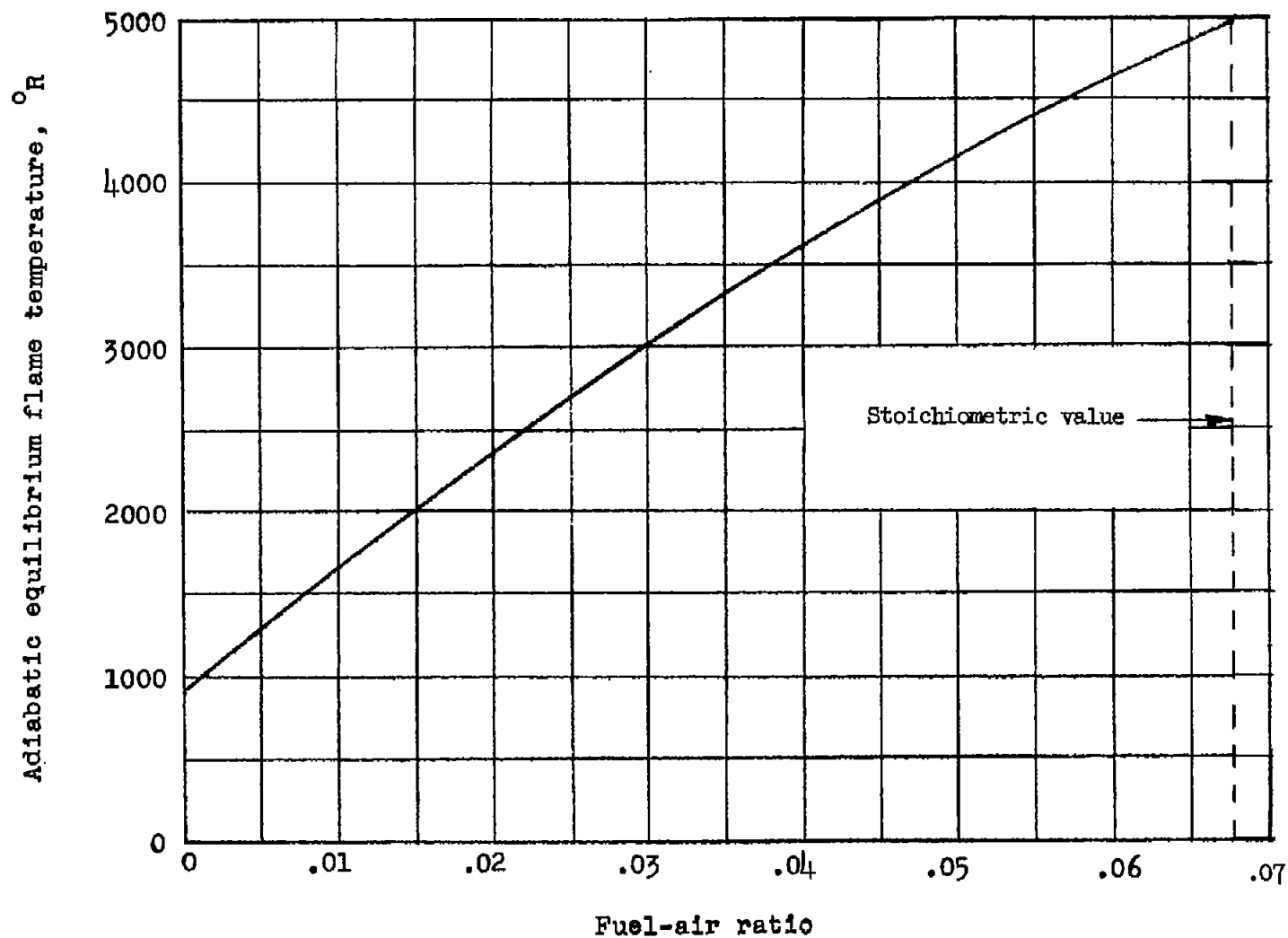


Figure 12.- Computed adiabatic equilibrium flame temperature from combustion of ethylene ( $C_2H_4$ ) fuel in air. Air preheat temperature,  $900^{\circ}R$ .

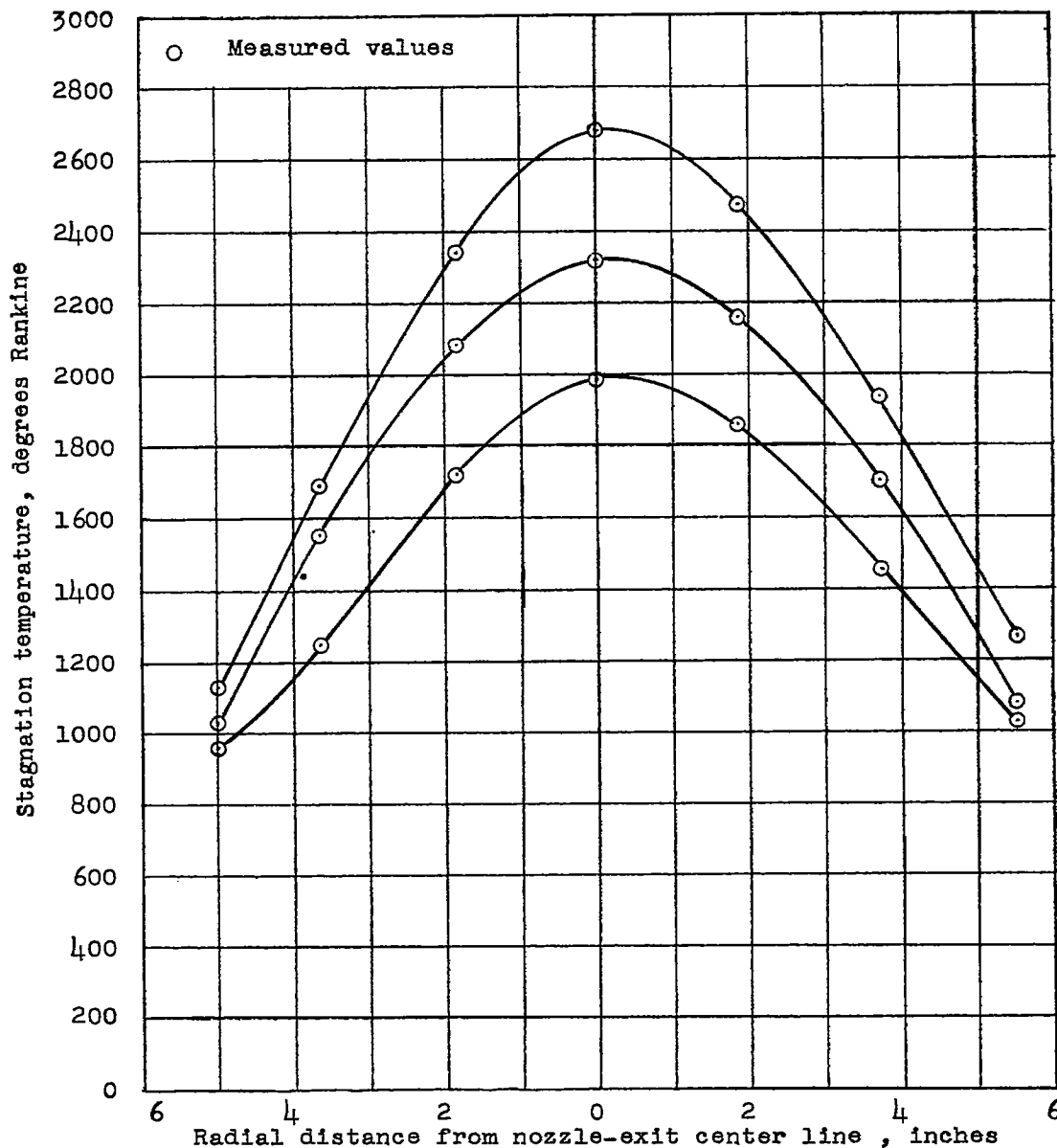


Figure 13.- Typical stagnation-temperature profiles across nozzle exit.

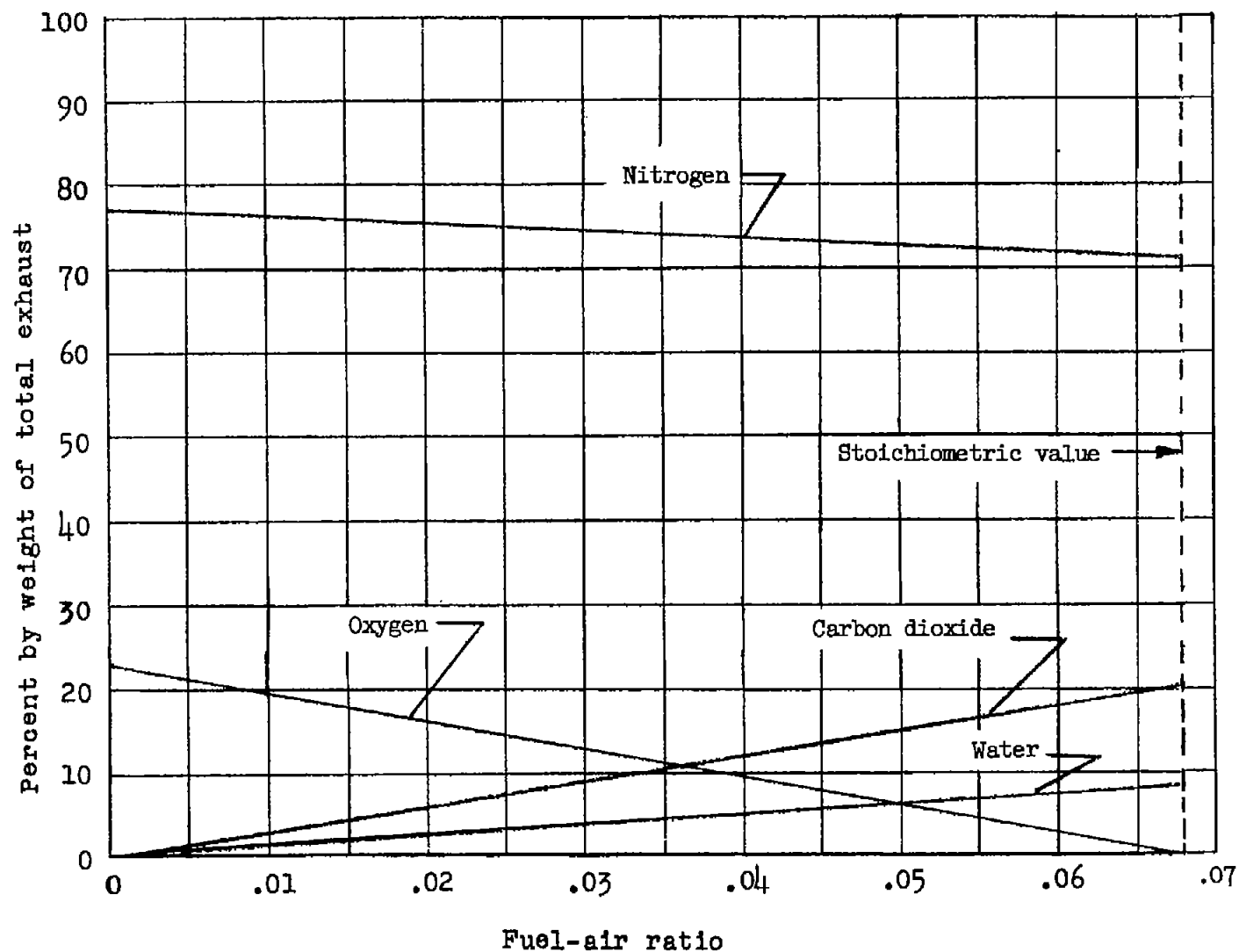
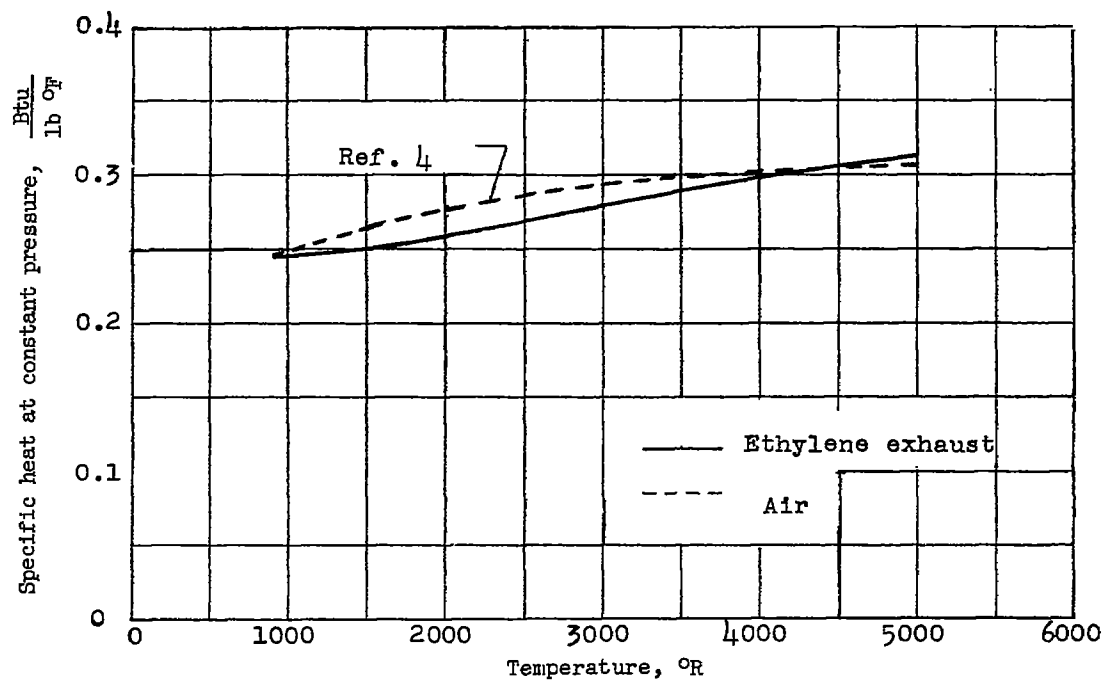
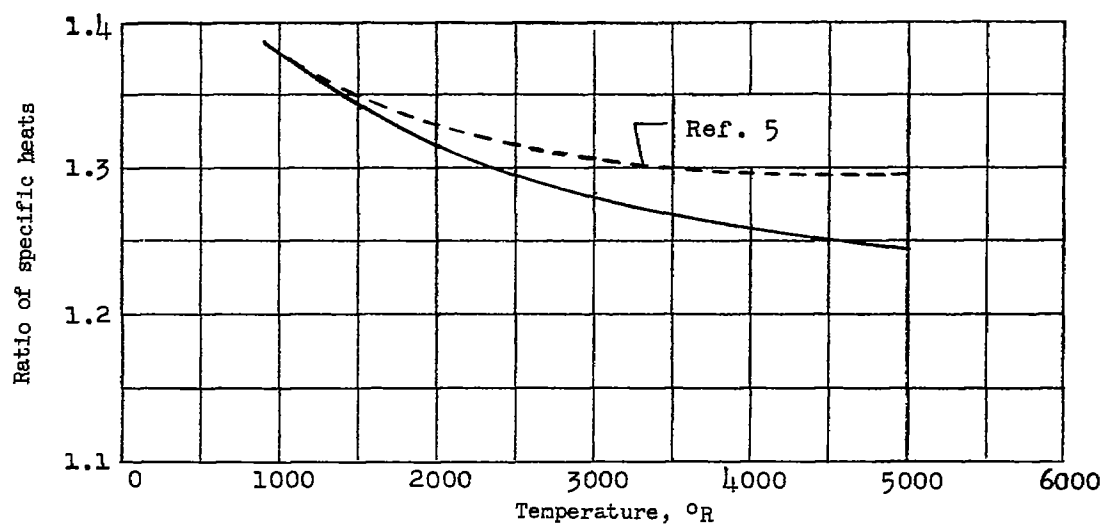


Figure 14.- Composition of exhaust from combustion of ethylene ( $C_2H_4$ ) in air.



(a) Specific heat at constant pressure.



(b) Ratio of specific heats.

Figure 15.- Ideal thermodynamic properties of ethylene exhaust as compared with air.